

A Detailed Model of Rear-Side Irradiance for Bifacial PV Modules

Clifford W. Hansen¹, Renee Gooding¹, Nathan Guay¹, Daniel M. Riley¹, Johnson Kallickal¹, Donald Ellibee¹, Amir Asgharzadeh³, Bill Marion², Fatima Toor³, Joshua S. Stein¹

¹Sandia National Laboratories, Albuquerque, NM, 87185-1033, USA

²National Renewable Energy Laboratory, Golden, CO, 80401, USA

³Electrical and Computer Engineering Department, The University of Iowa, Iowa City, IA, 52242, USA

Abstract — We describe and validate a method for modeling irradiance on the back surface of bifacial PV modules at the scale of individual cells using view factors. We compare model results with irradiance measurements on the back of PV modules in various configurations. Our analysis illustrates the relative accuracy of the model as well as the potential variation in back surface irradiance among the cells.

Index Terms — bifacial PV module, irradiance, view factor.

I. INTRODUCTION

Bifacial photovoltaic (PV) cells, modules, and systems potentially offer a pathway to significantly lower leveled cost of energy. Bifacial PV arrays are not widely deployed in part because their potential performance advantages are not generally understood. Sandia National Laboratories (Sandia), the National Renewable Energy Laboratory and the University of Iowa are investigating bifacial PV performance and characterization in a joint project funded by the US Department of Energy [1]. The project's main objectives are (1) measure the performance of various bifacial PV technologies using an outdoor test bed, (2) develop and validate models of back surface irradiance, and (3) work with industry to develop rating standards for bifacial PV modules. The outdoor test bed at Sandia in Albuquerque, NM allows investigation of the many factors that influence bifacial PV performance, including ground albedo and array geometry (e.g., height above ground, tilt angle, row position, row-to-row spacing).

Conceptually, total irradiance on the back surface of a rack-mounted module results from the combination of:

- Sky diffuse irradiance. The visible sky depends on the module's tilt and azimuth and is restricted by other nearby structures.
- Ground-reflected irradiance which can vary across the surfaces behind the module due to albedo and the irradiance incident on the ground surfaces.
- Structure-reflected irradiance from nearby objects such as from the front of PV modules in an adjacent row.
- Direct irradiance on the back surface, e.g., when the sun elevation is low and the sun azimuth is to the northeast or northwest of a south-facing array.

Accurate calculation of back surface irradiance remains a challenge. Previously [2] we compared two approaches to modeling back surface irradiance: view factor and ray tracing,

with view factor models considering either 3D or a simplified 2D array geometry. At the time, ray tracing models were computationally prohibitive for simulating energy production from bifacial PV arrays. View factor models with simplified 2D geometry cannot represent the full variation of irradiance among the cells in a row of bifacial PV modules, and hence the effect of this variation remains unquantified.

In this paper, we present and validate a computationally efficient approach for modeling back surface irradiance at single-cell resolution using view factors. Our approach represents the spatial non-uniformity in irradiance on the back surface by computing irradiance for each cell in a bifacial PV module.

II. MEASURED BACK SURFACE IRRADIANCE

Sandia National Laboratories is using reference cells to measure rear surface irradiance at high spatial resolution using a sensor array with the form factor of a single PV module (Fig.1) mounted in a variety of tilts and heights. We also measure front and back surface irradiance in conjunction with measuring bifacial PV module I-V curves mounted on several arrays. Fig. 2 illustrates a south-facing rack adjustable in height and tilt with monofacial PV modules on the west half (left in figure) and bifacial PV modules on the right half. Reference cells measure irradiance along the middle of the rack: at the top and bottom of the front, and at the top, middle and bottom of the rear. Reference cells are calibrated outdoors against a primary reference cell (calibrated by NREL) to reduce variation among cells to less than 4 W/m² at irradiance of 1000 W/m².

III. BACK SURFACE IRRADIANCE MODEL

Our back surface irradiance model uses view factors defined at the resolution of a single cell. Calculation of view factors at a cell level permits an array performance model to directly account for mismatch conditions among cells and modules, and also to represent arrays with subsets of modules in different configurations, e.g., a mix of southward facing, fixed tilt modules and vertical E-W facing modules. Compared to ray tracing simulations, this detailed view factor model is less demanding computationally and require fewer parameters but also represents a PV system with less detail. View factors can

be used to efficiently model irradiance for large, regular arrays (e.g., [3]) at the loss of detail regarding the variation in irradiance along the array's rows and at row ends.



Fig. 1. Movable sensor array for high spatial resolution measurements of rear-surface irradiance.



Fig. 2. Adjustable PV array at Sandia's Photovoltaic Systems Evaluation Laboratory.

III.A Detailed View Factor Model

View factors, also termed shape and configuration factors, quantify the fraction of irradiance reflected from one surface that arrives at a receiving surface. View factor models [4], [5] calculate back surface irradiance E_2 (W/m^2) by:

$$E_2 = \alpha \times G_1 \times F_{1 \rightarrow 2} \quad (1)$$

where G_1 is the total irradiance (W/m^2) on the reflecting area being considered (e.g., an area of the ground), α is the albedo of the reflecting surface and $VF_{1 \rightarrow 2}$ is the view factor (unitless) from the reflecting area to the receiving surface. The total irradiance on the back surface of a cell is the sum over all contributing reflecting surfaces. A rear surface irradiance model is then assembled by specifying the set of reflecting surfaces, albedos and the irradiance incident on each surface (Fig. 3).

A view factor model assumes that all reflecting surfaces are Lambertian, i.e., irradiance is scattered isotropically. An emitting surface (dA_1) reflects incident irradiance, part of which is incident on the receiving surface: the view factor $F_{1 \rightarrow 2}$ quantifies the fraction of irradiance emitted by A_1 that is received by A_2 . Formally, view factors are calculated by integration (Eq. 2) using terms in the illustration.

$$F_{1 \rightarrow 2} = \frac{1}{A_1} \int_{A_1} \int_{A_2} \frac{\cos \theta_1 \cos \theta_2}{\pi S^2} dA_2 dA_1 \quad (2)$$

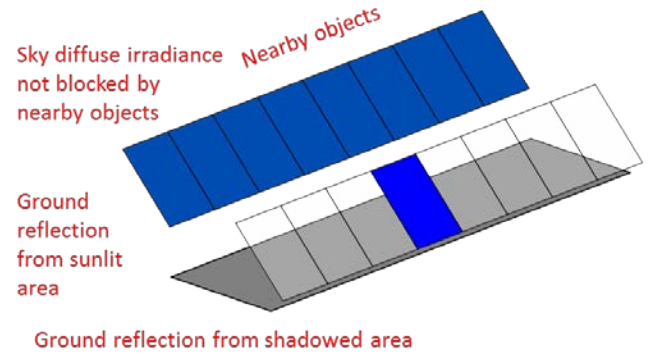


Fig. 3. Features in the detailed view factor model.

Our detailed view factor model calculates irradiance $E_{back}(t)$ at time t on the rear surface of cell k from DHI and DNI by

$$E_{back,k}(t) = E_{ground,k}(t) + E_{sky}(t)VF_{k \rightarrow sky} + E_{beam}(t) \quad (3)$$

$$E_{ground,k}(t) = \sum_i \alpha_i G_i(t) VF_{i \rightarrow k} \quad (4)$$

$$G_i(t) = DHI(t)VF_{i \rightarrow sky} + \delta_i(t)DNI(t)\cos(Z(t)) \quad (5)$$

$$E_{sky}(t) = \left[(1-A)DHI(t) \left(\frac{1 - \cos(\theta_r)}{2} \right) \right] \quad (6)$$

$$A = DNI(t)/H_o(t)$$

$$E_{beam}(t) = DNI(t)\cos(AOI(t))IAM(AOI(t)) \quad (7)$$

where i enumerates the reflecting surfaces, Z is the solar zenith angle, θ_r is the tilt from horizontal of cell k , $\delta_i(t) = 1$ if surface i is sunlit at time t and $\delta_i(t) = 0$ otherwise. Eq. 6 is obtained from the Hay and Davies model [6] for sky diffuse irradiance on a tilted surface by omitting its term for circumsolar diffuse irradiance; $H_o(t)$ is the extraterrestrial normal irradiance. In Eq. (7) $IAM(AOI(t))$ reduces any direct

irradiance on the rear surface of the cell for specular reflections; we use [7] with $a = 0.18$.

III.B Improving Computational Efficiency

We reported previously [2] on results from a partial implementation in MatlabTM of parts of the detailed view factor model (Algorithm A). Our earlier work assumed $VF_{k \rightarrow sky} = 1$, i.e., sky diffuse irradiance was not blocked by nearby objects. Our code was too slow for analysis of bifacial energy production (e.g., 15-minute time steps for a simulation year), nor for optimizing power production when varying bifacial PV module orientation and tilt.

Algorithm A: Inefficient algorithm for view factor model.

1. Compute solar positions and irradiance for all time steps.
2. For each time step:
 - a. Use the sun vector to project structures to shadows on the reflecting surfaces.
 - b. For sunlit and shaded areas of each surface, compute view factors to each cell using Eq. 2.
 - c. Compute irradiance on the rear surface of each cell using Eq. 1.

Analysis of Algorithm A shows two inefficiencies:

- View factors are recomputed at each time step, requiring numerical integration to converge for each cell and each reflecting area. This is highly inefficient because a view factor is a geometric quantity (Eq. 2) which has no dependence on the sun position.
- Numerical integration using the packaged MatlabTM function `integral2` is done separately for each cell, and is not amenable to vectorization for a list of cells.

To reduce computation time, we implement Algorithm B. We grid each reflecting surface in order to approximate the integrand $I(s, n_1, n_2)$ in the calculation of $VF_{i \rightarrow k}$ with its value $I(\hat{S}, n_1, n_2)$ at the midpoints of the reflecting and receiving cells. Moreover, calculation of $I(\hat{S}, n_1, n_2)$ can be expressed in terms of matrix operations only:

$$I(s) = \frac{\cos \theta_1 \cos \theta_2}{\pi s^2} \quad (7)$$

$$I(\hat{S}) = \frac{\langle \hat{S}, n_1 \rangle \langle -\hat{S}, n_2 \rangle}{\pi \|\hat{S}\|^2} = \frac{\hat{S}^T [-n_1 n_2^T] \hat{S}}{\pi \langle \hat{S}, \hat{S} \rangle^2} \quad (8)$$

Numerical exploration of a wide range of reflecting and receiving cell geometries revealed a rather complex relationship between cell dimensions and the approximation error $|I(s, n_1, n_2) - I(\hat{S}, n_1, n_2)|$. A rough rule of that sets

cell dimension $< 0.25 \|\hat{S}\|$ maintains approximation error $< 1\%$ except when cell normal vectors are nearly parallel. We set the grid boundaries at the intersection with the ground of a ray at an angle of 88° from a vertical ray from the cell's center to the ground. The resulting grid encompasses 97% or more of ground-reflected irradiance which might affect a receiving cell.

Algorithm B: Faster implementation of view factor model.

For each cell k :

1. Grid each reflecting surface.
2. For each combination of grid cell and module cell, compute $VF_{i \rightarrow k}$ using Eq. 3.
3. Compute solar positions and $E_{sky}(t)$ (Eq. (6)) for all time steps.
4. Compute $VF_{k \rightarrow sky}$.
5. For each time step:
 - a. Use the sun vector to project structures to shadows on the reflecting surfaces.
 - b. Identify each grid cell as having shaded or unshaded conditions (evaluate $\delta_i(t)$).
 - c. Return irradiance on the rear surface of the evaluation of Eq. (3), (4) and (5).

The expression in Eq. 8 involves a set of linear algebra operations which are computed once for each pair of reflecting and receiving cells. The implementation of Algorithm B using Eq. 8 can be done (using CUDA) for GPU rather than CPU processing, further reducing calculation time.

A computational test case using three receiving cells, a grid of 713×713 reflecting cells, ten objects which cast shadows and 151 time steps was used for timing analysis. The test case calculated irradiance at the three receiving cells at each time step. CPU processing took approximately 123 seconds to complete while the GPU implementation of the same algorithm completed in 14 seconds. For both implementations the largest amount of computation time is spent in step 5b, where the boundary of each object's shadow is traversed clockwise to determine grid cells whose centers lie to the right of every boundary segment.

IV. ANALYSIS

Fig. 4 compares modeled and measured irradiance at the 6 outer reference cells on a clear day, with the sensor array mounted on open racking (Fig. 1) at 30° tilt and 0.6m from the ground with a relatively clear view of the northern horizon and away from any objects with shadows that might cast shadows near the sensor array. Ground albedo is 0.23 measured with a Kipp and Zonen CMA-11 albedometer. At noon modeled irradiance is within 10 W/m^2 of measurement. The skewed

curves for the middle and bottom rows result from the sensor array's shadow passing underneath the sensor array.

Fig. 5 shows model residuals for each of the 10 cells. Model predictions are generally within 15 W/m² (8%) around solar noon, and within 20 W/m² at all times. Explanation for the observed negative bias (model < measured) has so far proven elusive. Possible causes include:

1. code errors;
2. error in the sky diffuse irradiance model ([6] in this case) which is used to estimate irradiance incident on shadowed areas on the ground (ground reflections comprise essentially all of irradiance in Fig. 4).
3. spectral changes in irradiance reflected from ground surfaces;
4. deviation from the assumption that reflections are Lambertian.

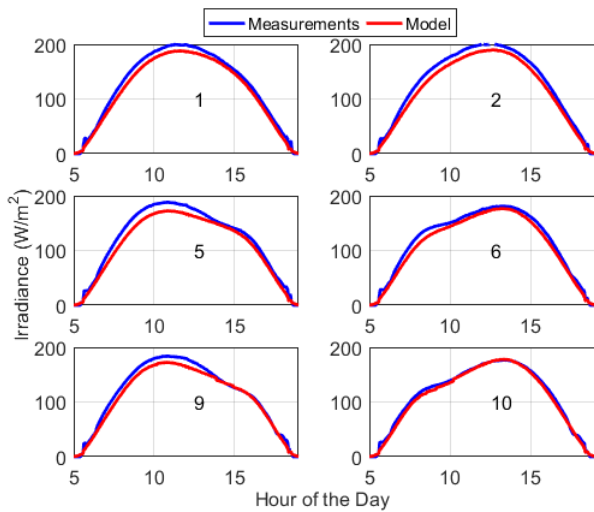


Fig. 4. Modeled and measured rear irradiance for six outside cells in the sensor array: May 5, 2017, a clear day, isolated open rack mount tilted at 30°.

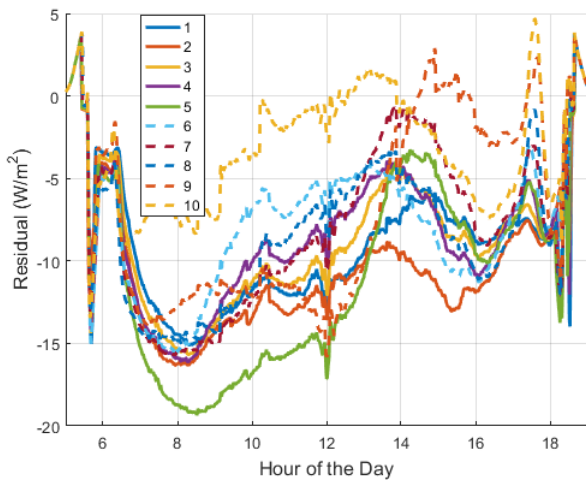


Fig. 5. Model residuals for all 10 cells in the sensor array: May 5, 2017.

Fig. 6 compares measured and modeled irradiance at all times for three days with different conditions (broken clouds persisted through April 30 morning, and May 2 afternoon; otherwise clear sky conditions obtained). For May 2 and May 5, the negative bias is evident. For April 30 morning, a positive bias of approximately 20 W/m² is observed (Fig. 7). The variation in prediction bias from -15 W/m² (May 5, Fig. 5) to 20 W/m² (April 30, Fig. 7) gives a rough envelope of model accuracy for all sky conditions of about ±10%.

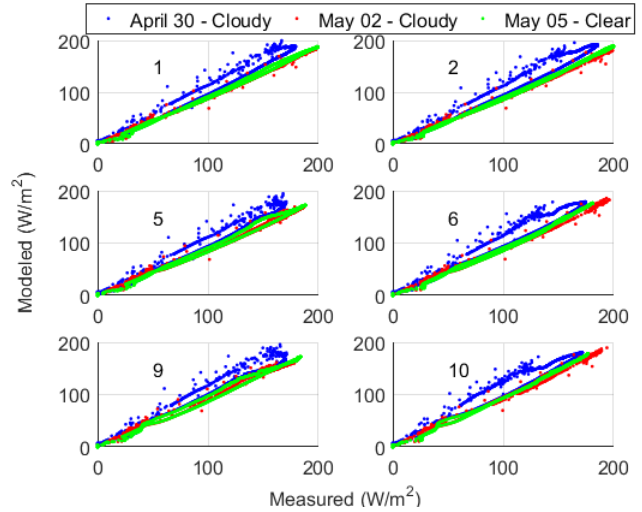


Fig. 6. Modeled and measured rear irradiance for six outside cells in the sensor array: varied sky conditions, isolated open rack mount tilted at 30°.

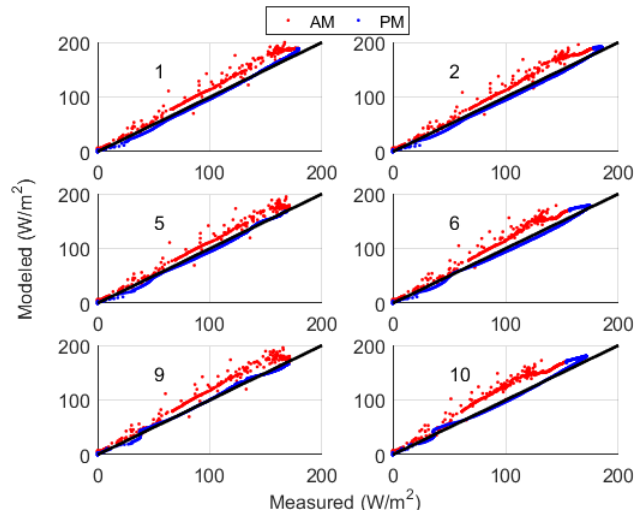


Fig. 7. Modeled and measured rear irradiance for six outside cells in the sensor array: April 30, 2017, isolated open rack mount tilted at 30°. Black line is 1:1.

Fig. 8 compares modeled and measured irradiance at the 6 outer reference cells on a clear day, with the sensor array mounted vertically on isolated racking in landscape orientation 0.63m from the ground. The array is mounted above a concrete block with no gap in between the block and array to keep the

shadow shape simple. Direct irradiance on the rear surface of the sensor array cause the ‘ears’ in each trace; reflection off a nearby row of PV modules appears as a spike just before the afternoon ‘ear’. Model results are within 20 W/m² of measurements, with a similar negative bias as is observed for the sensor array on tilted racking.

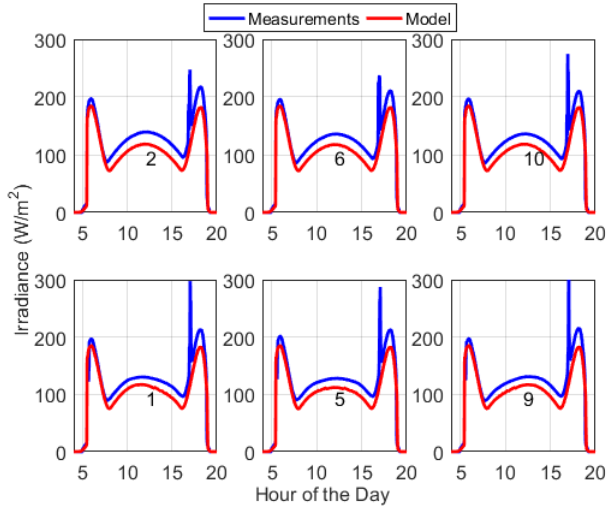


Fig. 8. Modeled and measured rear irradiance for six outside cells in the movable sensor array: May 20, 2017, a clear day, vertical isolated open rack mount.

We simulate irradiance at the three rear-facing reference cells on the adjustable array shown in Fig. 2. These simulations account for shadows cast by the four modules and the array frame structure as depicted in Fig. 9. Fig. 10 and Fig. 11 compare modeled and measured irradiance for clear day with the array at relatively steep and shallow tilt, respectively. The shape evident for the bottom cell results from the passage of the array’s shadows below the cell: the morning and afternoon shoulders correspond to shadows from the modules falling beneath the cell, and the midday peak from the sunlight passing through the gap between the modules.

The model reproduces the shapes evident for each reference cell indicating that the view factor method generally captures the effects of shadows on ground-reflected irradiance. A systematic bias towards underestimating irradiance by approximately 15 W/m² is observed for periods of time (early/late hours) or reference cells (top) for which array shadows do not significantly affect the received irradiance. The consistency of the bias, and the absence of dependence on time of day, suggest the explanation lies with the sky diffuse irradiance model or a reduction in spectral irradiance to which the reference cells respond. If the bias was due to an incorrect value for the ground albedo, we would expect the bias to affect all reference cells in a similar manner, and the discrepancy between model and measurement to shrink at lower irradiance: neither effect is apparent in Fig. 10. The roughness of the model curves results from projecting array shadows onto the grid used

for computing view factors, resulting in pixelated shadow boundaries.

Fig. 11 compares modeled and measured irradiance for a clear day with the array at 15° tilt, where nearly all of the received rear-surface irradiance results from ground reflection. Shadows from the array affect all three reference cells. Model bias remains evident although smaller in magnitude than with the steeply tilted configuration.

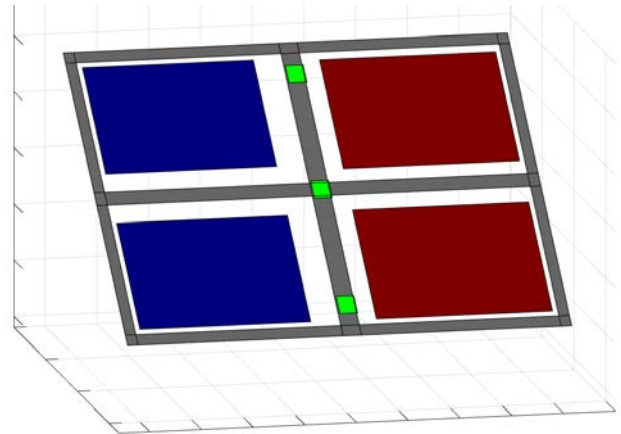


Fig. 9. Schematic of adjustable array features represented in rear irradiance model. Blue: monofacial modules, red: bifacial modules, green: reference cells (facing away), grey: structure.

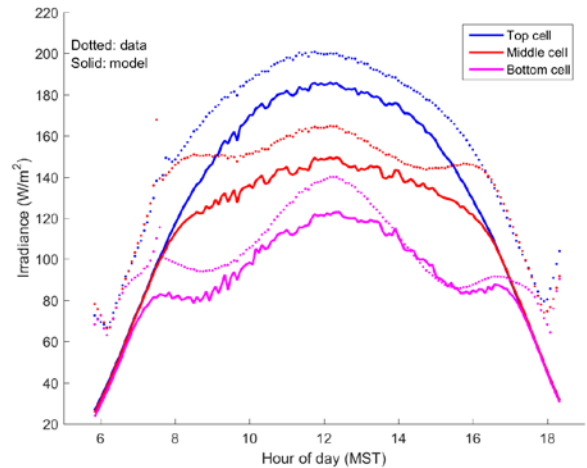


Fig. 10. Modeled and measured irradiance for rear-facing reference cells in the adjustable array: 16 June 2016, a clear day, array titled at 45° with center at 1.63m above ground.

Fig. 12 illustrates the cell-to-cell variation in modeled irradiance for the top-right bifacial module (6 × 10 cells in landscape orientation). The model predictions show a variation as great as 50 W/m², or roughly 5% of total irradiance (front and back) on the bifacial module. The modeled cell-to-cell variation is informative for efforts to develop performance models for bifacial PV modules (e.g. [8]) as this variation contributes to power losses due to mismatched output between cells in series. It is anticipated that cell-to-cell variation widens

with increasing albedo, and decreases with increasing height above ground, in conjunction with increased rear-surface irradiance and decreasing view factors, respectively [9].

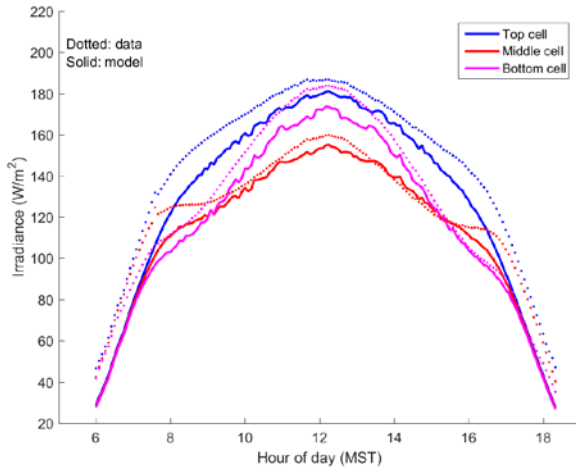


Fig. 11. Modeled and measured irradiance for rear-facing reference cells in the adjustable array: 14 July 2016, a clear day, array tilted at 15° with center at 1.63m above ground.

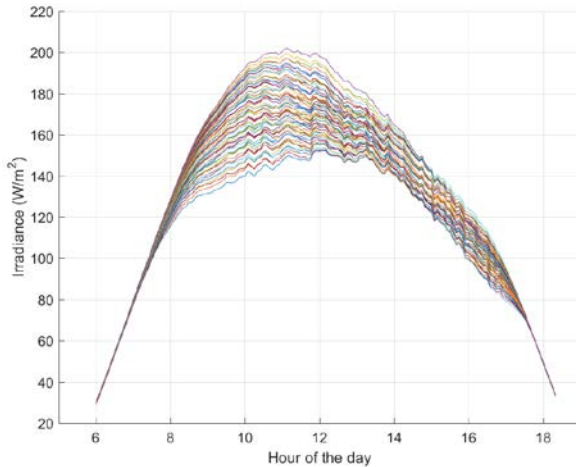


Fig. 12. Modeled rear irradiance by cell on the top right bifacial module in the adjustable array: 6 July 2016, a clear day, array tilted at 15° with center at 1.63m above ground.

V. CONCLUSIONS

We present and show validation for a detailed model of rear-surface irradiance at the scale of individual cells. Our model operates on DNI, DHI, albedo and system geometry as input. Irradiance reaching the back surface of a cell is computed as the sum over ground reflections (accounting for shadows on the ground from nearby objects), sky diffuse irradiance and direct irradiance. Within the validation presented, our model shows an accuracy of roughly $\pm 10\%$ when compared to irradiance measured with reference cells.

This detailed rear irradiance model, in its present MatlabTM implementation, is useful for analysis of module- and string-scale performance of bifacial PV systems. Computation time for larger systems remains a challenge: simulating two 6×10 cell modules (total of 120 receiving cells) with 10 shadow-casting objects for 100 time steps requires about 5 minutes using CPU processing. Computation time can be dramatically reduced when GPU processing is available, and the algorithm can easily be parallelized.

ACKNOWLEDGEMENTS

This work was supported by the U.S. Department of Energy SunShot Initiative. Sandia National Laboratories is a multi-program laboratory managed and operated by Sandia Corporation, a wholly owned subsidiary of Lockheed Martin Corporation, for the U.S. Department of Energy's National Nuclear Security Administration under contract DE-AC04-94AL85000.

REFERENCES

- Stein, J., C. Deline, and F. Toor. *Outdoor Field Performance from Bifacial Photovoltaic Modules and Systems*. in *44th IEEE Photovoltaic Specialist Conference*, 2017. Washington, DC.
- Hansen, C.W., et al. *Analysis of Irradiance Models for Bifacial PV Modules*. in *43rd IEEE Photovoltaic Specialist Conference*, 2016. Portland, OR.
- Marion, B., et al. *A Practical Irradiance Model for Bifacial PV Modules*. in *44th IEEE Photovoltaic Specialist Conference*, 2017. Washington, DC.
- Iqbal, M., *An Introduction to Solar Radiation*. 1983, Toronto: Academic Press Canada.
- Yusufoglu, U.A., et al., *Simulation of Energy Production by Bifacial Modules with Revision of Ground Reflection*. *Energy Procedia*, 2014. **55**: p. 389-395.
- Hay, J.E. and J.A. Davies. *Calculations of the solar radiation incident on an inclined surface*. in *First Canadian Solar Radiation Data Workshop*, 59, 1980. Ministry of Supply and Services, Canada.
- Martin, N. and J.M. Ruiz, *Calculation of the PV modules angular losses under field conditions by means of an analytical model*. *Solar Energy*, 2001. **70**: p. 25-38.
- Riley, D., et al. *A Performance Model for Bifacial PV Modules*. in *44th IEEE Photovoltaic Specialist Conference*, 2017. Washington, DC.
- Krein, L., et al. *PV module power gain due to bifacial design. Preliminary experimental and simulation data*. in *2010 35th IEEE Photovoltaic Specialists Conference*, 2010.